Average properties of the magnetic reconnection ion diffusion region in the Earth's magnetotail: The 2001–2005 Cluster observations and comparison with simulations

J. P. Eastwood,[1,2] T. D. Phan,[1] M. Øieroset,[1] and M. A. Shay[3]

Received 2 October 2009; revised 11 December 2009; accepted 4 February 2010; published 14 August 2010.

[1] Magnetic reconnection plays a key role in the circulation of plasma through the Earth's magnetosphere. As such, the Earth's magnetotail is an excellent natural laboratory for the study of reconnection and in particular the diffusion region. To address important questions concerning observational occurrence rates and average properties, the Cluster data set from 2001–2005 has been systematically examined for encounters with reconnection X lines and ion diffusion regions in the Earth's magnetotail. This survey of 175 magnetotail passes resulted in a sample of 33 correlated field and flow reversals. Eighteen events exhibited electric and magnetic field perturbations qualitatively consistent with the predictions of antiparallel Hall reconnection and could be identified as diffusion region encounters. The magnitudes of both the Hall magnetic and electric field were found to vary from event to event. When normalized against the inflow magnetic field and the current sheet number density the average peak Hall magnetic field was found to be 0.39 ± 0.16, the average peak Hall electric field was found to be 0.33 ± 0.18, and the average out of plane (reconnection) electric field was found to be ~0.04. Good quantitative agreement was found between these results and a large, appropriately renormalized particle-in-cell simulation of reconnection. In future missions, the magnitude of the total DC electric field may be a useful tool for automatically identifying ion diffusion region encounters.

Citation: Eastwood, J. P., T. D. Phan, M. Øieroset, and M. A. Shay (2010), Average properties of the magnetic reconnection ion diffusion region in the Earth's magnetotail: The 2001–2005 Cluster observations and comparison with simulations, *J. Geophys. Res.*, *115*, A08215, doi:10.1029/2009JA014962.

1. Introduction

[2] Magnetic reconnection is a universal plasma process that is important in many different physical phenomena. In the context of the Earth's magnetosphere, collisionless reconnection plays a key role in transporting energy and solar wind plasma across the magnetopause and through the magnetotail [*Dungey*, 1961; *Fairfield and Cahill*, 1966]. As such, the magnetosphere is an excellent natural laboratory for in situ studies of reconnection physics, particularly the diffusion region where the magnetic field decouples from the plasma, allowing previously separate regions to mix.

[3] An important development in the theory of magnetic reconnection has been the prediction that the diffusion region should exhibit a characteristic two-scale structure due to differential ion (proton) and electron motion [e.g., *Sonnerup*, 1979; *Shay et al.*, 1998; *Birn et al.*, 2001]. The heavier protons decouple from the magnetic field at a larger scale than the electrons in the so-called ion diffusion region, whereas the electrons decouple, and the magnetic field reconnects, in the electron diffusion region. This gives the ion diffusion region a characteristic structure, as shown in Figure 1. The diffusion region is expected to be observed in the context of a correlated reversal in the normal magnetic field (B_z) and the direction of plasma outflow (v_x). The magnetic field **B** has a quadrupole structure in the out-of-plane direction (B_y), and the electric field **E** has a bipolar structure in the direction normal to the current sheet (E_z). Note that in this picture, there is no guide field ($\langle B_y \rangle = 0$) and the boundary conditions above and below the current sheet are symmetric. The Hall magnetic field is also associated with Hall currents that can be observed further from the diffusion region.

[4] The first pieces of experimental evidence supporting this two-scale model were based on observations of Hall currents and Hall fields along the separatrices [*Fujimoto et al.*, 1997; *Nagai et al.*, 2001] as well as in the vicinity of the diffusion region in the Earth's magnetopause and magnetotail [*Øieroset et al.*, 2001; *Mozer et al.*, 2002]. Further observations from Geotail provided important information concerning the typical location of magnetotail reconnection

[1]Space Sciences Laboratory, University of California, Berkeley, California, USA.
[2]Now at Blackett Laboratory, Imperial College London, London, UK.
[3]Department of Physics and Astronomy, Bartol Research Institute, University of Delaware, Newark, Delaware, USA.

0148-0227/10/2009JA014962

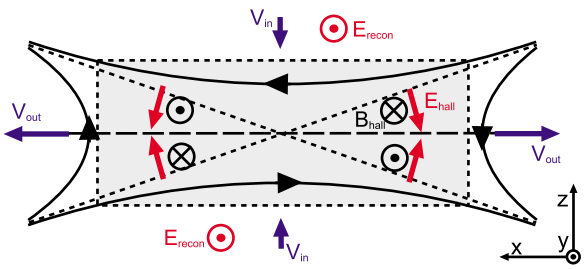

Figure 1. The basic theoretical structure of the diffusion region. The magnetic fields are shown in black, electric fields in red, and plasma flow in blue. The coordinate system corresponds to Geocentric Solar Magnetospheric (GSM). In diffusion regions in the Earth's magnetotail, outflow jets point along the x direction, the quadrupole Hall magnetic field is usually observed in the y direction, and the bipolar Hall electric field is usually observed in the z direction.

(identified by the simultaneous reversal of B_z and v_x) [*Nagai et al.*, 1998; *Nagai et al.*, 2005] and the pattern of the Hall currents during substorm onset [*Nagai et al.*, 2003; *Asano et al.*, 2004].

[5] More recently, exploration of the diffusion region has mainly used data from the multispacecraft Cluster mission [*Escoubet et al.*, 2001], principally in a series of individual event case studies as summarized by *Paschmann* [2008], who provides a good overview of recent activity in this area. Cluster has made extensive observations of the magnetotail, and a number of magnetotail diffusion region encounters have been reported. In this context, the diffusion region that has received the most attention was observed on 1 October 2001, 0947 UT–0952 UT. The properties of the Hall magnetic field [*Runov et al.*, 2003], Hall electric field [*Wygant et al.*, 2005], energetic particles [*Imada et al.*, 2007; *Chen et al.*, 2008], and electrostatic structures [*Cattell et al.*, 2005] have all been examined. Four other completely measured (i.e., magnetic and electric field) diffusion regions have been studied by *Borg et al.* [2005], *Eastwood et al.* [2007, 2009], and *Runov et al.* [2008], who in particular noted that the electric field measurements are important in determining whether the ions are frozen in. Other diffusion region events have been studied based on the Hall magnetic field alone [*Alexeev et al.*, 2005; *Henderson et al.*, 2006; *Nakamura et al.*, 2006; *Laitinen et al.*, 2007; *Xiao et al.*, 2007]. *Asano et al.* [2008] examined three diffusion region events in detail and performed a survey looking for intervals of flat top electron distributions that occur in conjunction with reconnection, finding 13 intervals. Also, *Østgaard et al.* [2009] have studied the relationship between reconnection and auroral intensifications, using the signature of the Hall magnetic field to establish the presence of 13 reconnection events in the magnetotail. However, this work was aimed at identifying different candidate magnetospheric events for study rather than establishing the average properties of the diffusion region itself.

[6] A number of open questions remain as a result of these studies. The first concerns the statistics of diffusion regions encounters. Whether a spacecraft encounters a diffusion region in the magnetotail is ultimately a matter of chance. Since the diffusion region itself is thought to be relatively small (the ion inertial length $c/\omega_{pi} \sim 700$ km if $n = 0.1$ cm^{-3}), encounters are generally considered to be fairly rare. However, it is unclear as to whether the existing set of published Cluster magnetotail observations constitutes the entire set of encounters. Second, in the magnetotail the macroscopic signatures of reconnection are fast Earthward flow correlated with northward magnetic field and fast tailward flow correlated with southward magnetic field [*Baumjohann et al.*, 1990; *Ueno et al.*, 1999]. While individual diffusion regions such as those cited above have been shown to occur in the vicinity of field and flow reversals, what is the likelihood that a specific observation of macroscopic reconnection signatures (i.e., a flow reversal) also corresponds to an encounter with the ion diffusion region? Third, it is possible that thus far, only the largest events (for example those with the biggest Hall field perturbation, or largest reconnection rate) have been studied. Do the reported diffusion regions, taken together, represent the average? Finally, as yet there has been no effort (to our knowledge) to synthesize these different studies into an average experimental picture of the diffusion region in the magnetotail that can be compared with simulations and theory. Furthermore, while the answers to these questions are of intrinsic importance to improving our understanding of magnetic reconnection, they are also useful on a more practical level for the planning of future missions, such as Magnetospheric Multiscale and cross-scale, or any future magnetospheric constellation mission.

[7] In this paper, the results of a survey of the Cluster data set for magnetotail diffusion region encounters are presented, with the aim of addressing the above questions. The Cluster data are presented in section 2, and in section 3 the survey of the data is presented. In section 4, we examine several average properties of the ion diffusion region for antiparallel reconnection, in particular the average Hall electric field, the average Hall magnetic field, and the reconnection electric field. The results are discussed and compared to simulations in section 5, and conclusions are presented in section 6.

2. Data

[8] The four identical Cluster spacecraft were launched in 2000 into coordinated polar orbits around the Earth with an apogee of 19.6 Re (Earth radii) and a perigee of 4 Re [*Escoubet et al.*, 2001]. For the first 4 years, the orbits were maintained so that apogee occurred near the ecliptic plane, (i.e., in the plasma sheet when in the magnetotail) and so that the spacecraft formed a regular tetrahedron at apogee. The scale of the tetrahedron was varied every 6 months, so for each tail season (~1 August–31 October) the spacecraft were at different separations (see Table 1). In 2005, the

Table 1. Properties of Cluster Data, by Year

Year	Tetrahedron Scale Size (km)	Number of Magnetotail Passes
2001	2000	36
2002	4000	38
2003	200	33
2004	1000	34
2005	10000/1000	34
		= 175

strategy was changed so Cluster 1, Cluster 2, and Cluster 3 formed a triangle of 10 000 km, and the separation between Cluster 3 and Cluster 4 perpendicular to the plane of the triangle was 1000 km. From 2005, the line of apsides was allowed to precess toward the South Pole so that when in the magnetotail, the spacecraft have crossed the plasma sheet closer and closer to the Earth during each successive tail season.

[9] In this study we have used magnetic field data from the Flux-Gate Magnetometer (FGM) experiment [*Balogh et al.*, 2001]. Four second period data have been used unless otherwise noted. Electric field data were measured by the Electric Field and Waves instrument (EFW) [*Gustafsson et al.*, 2001]. EFW uses four wire booms to measure two components of the electric field in the spin plane of the satellite (~x-y Geocentric Solar Ecliptic). The third component of the electric field has been reconstructed using the assumption that $\mathbf{E} \cdot \mathbf{B} = 0$, which is thought to hold everywhere except in the very small electron diffusion region (which is not the subject of this paper). This reconstruction requires that B_x/B_z and B_y/B_z are not too large, and that B_z itself is not too small, so errors in E_x and E_y are not amplified. In this study, the conditions $B_{x,y}/B_z < 10$ and $|B_z| > 1$ nT have generally been used. E_x data is shown at 4 s resolution; E_y and E_z are shown only when they can be reconstructed and so these time series tend to be irregularly sampled. Ion plasma data were measured by the Cluster Ion Spectrometry (CIS) Hot Ion Analyzer (HIA) experiment [*Rème et al.*, 2001], available on Cluster 1 and Cluster 3. All data are presented in the Geocentric Solar Magnetospheric (GSM) coordinate system unless otherwise noted.

3. Data Survey

3.1. Identification of Reconnection Events

[10] As mentioned in the previous section, during the latter part of the Cluster mission the line of apsides has been allowed to precess toward the South Pole, so the spacecraft cross the magnetotail current sheet at smaller and smaller radial distances from the Earth. Even during the 2005 tail season, it was found that dwell time of the spacecraft in the central plasma sheet was decreasing, and so here we have studied the first five tail seasons from 2001–2005. The orbital period is 57 h, and so during each 3-month tail season, on average Cluster observed 35 traversals of the magnetotail current sheet from the northern to the southern lobe, corresponding to a total of 175 observed magnetotail passes as shown in Table 1. Because of data gaps (due, for example, to eclipse intervals) and other operational issues, the number of observed magnetotail crossings is reduced in some years. It should be noted that this corresponds to the number of overall traversals due to orbital motion; the actual number of current sheet crossings is significantly greater.

[11] For each of these magnetotail passes, the data were split into 6 h long intervals and visually inspected using overview plots of the magnetic field strength and its components (from four spacecraft) and the plasma velocity components and the plasma β (from Cluster 1 and 3). All intervals where Cluster 1 and/or Cluster 3 encountered the plasma sheet, corresponding to an ion plasma β greater than or equal to 1 [*Baumjohann*, 1993], were retained. Each interval was then examined in more detail for events where Cluster 1 and/or Cluster 3 observed a significant Earthward or tailward flow ($|v_x| > \sim 100$ km s^{-1}) to reverse sign, accompanied by a correlated reversal in the sign of B_z, as would be expected for an X-line encounter (Figure 1). Flow reversals without a reversal in B_z were discarded, since they are often observed in association with bursty bulk flows (BBFs) and associated flow vortices [*Birn et al.*, 2004]. This resulted in a list of 33 events, shown in Table 2. Some flow reversals were not observed by both spacecraft, either because of data gaps or because one spacecraft was not located in the plasma sheet and did not observe the reconnection jets. In Table 2, the column Jet Obs. indicates whether the flow reversal was observed by Cluster 1 and/or Cluster 3. The stated duration of each event corresponds only to the central flow reversal. In many cases, high-speed flow was observed to persist for (tens of) minutes before and/or after the reversal. However, since we are interested in identifying the central diffusion region, we have restricted ourselves to identifying only the main reversal. A general remark arising from the survey is that Cluster observed numerous earthward BBFs and encountered more intervals of Earthward than tailward flow. This suggests that the average location of the reconnection region was tailward of the Cluster apogee of 19.6 Re, consistent with previous Geotail studies showing an average near-Earth X-line location of 20–30 Re [*Nagai et al.*, 1998; *Nagai et al.*, 2005].

[12] Although the expected macroscopic signature of a magnetotail reconnection X line is a correlated reversal in v_x and B_z, in an analysis of one particular field and flow reversal, Cluster data were used to show that this signature was in fact created by two X lines bounding an O line [*Eastwood et al.*, 2005]. We therefore used the multispacecraft Cluster data to examine each event in an attempt to establish whether the flow reversal was due to a crossing of an X line or an O line. The most reliable indication of a single X line observed by multiple spacecraft is that they simultaneously observe diverging jets at the center of the flow reversal. Thus we first examined the Cluster 1 and Cluster 3 plasma data for diverging plasma jets. However, there are several caveats. If they are too close together, there is no significant difference in the measurements of the two spacecraft. If they are too far apart, particularly in the z_{GSM} direction, it is possible that one spacecraft will remain at times outside of the reconnection jet. This means that in several examples, although the separation was potentially large enough in the *x-y* plane, separation in the *z* direction meant that there were no jet measurements enabling the bracketing of the X line.

[13] If it is not possible to establish the X-line geometry with the two spacecraft plasma data, the next step is to examine the four spacecraft magnetic field data at the time the flow reverses. For example, if the flow changes from tailward to Earthward, and if the spacecraft each observe B_z to change from negative to positive in an order consistent with their increasing distance from the Earth, then the encounter is identified as an X line. This allows the motion to be identified even if the flow reversal was observed only by one spacecraft. Again, if the spacecraft are too close together it is difficult to establish the X-line structure, particularly if there are waves also present. If the spacecraft are

Table 2. Intervals Where Cluster Encountered a Correlated Reversal in V_x and B_z in the Magnetotail Plasma Sheet ($\beta > 1$)[a]

Event	Date	Start	End	Jet Obs.	Multipoint Analysis		Inferred Structure		Diffusion Region?	Hall #
A	2001/08/13	02:55:00	02:59:00	1,3	X-line	Tailward			Inconclusive	
B	2001/08/22	09:43:00	09:45:00	1,3	X-line	Earthward			Yes	1
C	2001/08/22	09:50:00	09:57:00	1,3	–	–	X-line	Tailward	Yes	2
D	2001/08/27	04:03:00	04:07:00	1,3	X-line	Tailward			No	
E	2001/09/10	07:55:00	07:58:00	1,3	X-line	Tailward			Yes	3
F	2001/09/12	13:05:00	13:08:00	3	X-line	Tailward			Guide Field	
G	2001/09/12	13:10:00	13:13:00	3	X-line	Tailward			Guide Field	
H	2001/09/15	00:20:45	00:21:30	3	X-line	Earthward			Inconclusive	
I	2001/09/15	00:21:30	00:25:00	1,3	X-line	Tailward			Inconclusive	
J	2001/09/15	05:03:00	05:04:00	1	–	–	X-line	Earthward	Yes	4
K	2001/09/15	05:05:00	05:08:00	1,3	–	–	X-line	Tailward	Yes	5
L	2001/10/01	09:38:00	09:41:00	1,3	X-line	Tailward			Guide Field	
M	2001/10/01	09:47:00	09:51:00	1,3	X-line	Tailward			Yes	6
N	2001/10/08	12:52:00	12:59:00	1,3	X-line	Tailward			Yes	7
O	2001/10/11	03:28:00	03:37:00	1,3	–	–	X-line	Tailward	Yes	8
P	2002/08/18	17:07:00	17:09:00	1	X-line	Tailward			Yes	9
Q	2002/08/18	17:28:00	17:32:00	1	X-line	Tailward			Yes	10
R	2002/08/21	08:15:00	08:19:00	1,3	X-line	Tailward			Yes	11
S	2002/08/28	10:03:00	10:08:00	1	X-line	Tailward			Guide Field	
T	2002/09/18	13:09:00	13:15:00	3	–	–	X-line	Tailward	Yes	12
U	2002/10/02	21:20:00	21:21:00	1	X-line	Earthward			Inconclusive	
V	2002/10/02	21:21:00	21:22:30	1	X-line	Tailward			Yes	13
W	2002/10/26	09:18:00	09:21:00	3	–	–	X-line	Tailward	No	
X	2003/09/01	04:31:00	04:35:00	1,3	–	–	X-line	Tailward	Inconclusive	
Y	2003/09/19	23:29:00	23:31:00	1,3	–	–	X-line	Tailward	Yes	14
Z	2003/10/02	00:46:00	00:48:00	1,3	O-line	Earthward			No	
AA	2003/10/04	06:18:30	06:21:45	1,3	–	–	X-line	Earthward	Yes	15
AB	2003/10/09	02:23:00	02:27:00	1,3	–	–	X-line	Tailward	Yes	16
AC	2004/09/14	23:04:45	23:06:00	1	X-line	Tailward			Yes	17
AD	2004/10/03	18:14:00	18:17:00	1,3	X-line	Earthward			No	
AE	2004/10/11	00:35:30	00:37:00	1,3	–	–	X-line	Tailward	No	
AF	2005/08/28	23:40:00	23:43:30	3	X-line	Tailward			Guide Field	
AG	2005/09/26	09:43:00	09:51:00	1	–	–	X-line	Tailward	Yes	18

[a]The column Jet Obs indicates which spacecraft observed a reconnection jet. The column Multipoint Analysis indicates the results of the analysis described in section 3.1. The column Diffusion Region? indicates the qualitative agreement of the data with the expected pattern of Hall fields shown in Figure 1.

too far apart, then the decorrelated nature of the time series, together with waves and fluctuations, can in certain cases make it impossible to draw firm conclusions about the structure of the diffusion region at the time the flow reverses. However, in certain circumstances, the magnetic field is sufficiently well correlated, yet the spacecraft are far enough apart, to perform a timing analysis [*Schwartz*, 1998; *Eastwood et al.*, 2005] on the reversal in B_z, which ought to correspond to the plane separating Earthward and tailward flow. Hence it is possible to determine observationally whether the field and flow reversal corresponds to an X-line or an O-line crossing.

[14] As shown in Table 2, in 21 of the 33 events the multispacecraft data could be used to determine the qualitative structure of the magnetic field (column Multipoint Analysis). Of these 21 events, 20 were found to correspond to an encounter with a single X line. Only one, the previously studied event observed on 2 October 2003 [*Eastwood et al.*, 2005], was found to be consistent with an O line as opposed to a single X line. The time series for this event is unusual in the context of all the other events we have studied. The reversal in B_z is sharp and smooth and the flows are steady on both sides. Therefore, in the majority of cases that can be studied, a field and flow reversal appears to be consistent with a single X line. In the cases where multispacecraft data could not be used to determine the X-line structure, we proceed on the basis that they are highly likely to be a single X-line encounter; these events and the direction of X-line motion are shown in Table 2 in the column Inferred Structure.

[15] We now make some more general comments about the data set. Of the 32 X-line events, 6 showed a positive to negative reversal in v_x (i.e., an X line moving Earthward) and 26 showed a negative to positive reversal, meaning that at the location of Cluster, X lines are more often observed to move tailward. On four occasions, a +/− reversal was followed within a few minutes by −/+ reversal, consistent with an X line moving Earthward and then retreating tailward. On two occasions, two tailward moving X lines were observed within a few minutes of each other. This indicates that multiple X-line reconnection does occur in the magnetotail but that such observations are rare.

3.2. Identification of the Ion Diffusion Region

[16] Having established the basic nature of each of the 33 encounters described in the previous section, we then examined the structure of both the magnetic and electric field in more detail. In several previous studies the GSM coordinate system has been found to be generally appropriate for all analysis [*Runov et al.*, 2003; *Borg et al.*, 2005; *Eastwood et al.*, 2007], and its use is an appropriate starting point for this analysis. In some cases the geometry could be rotated relative to GSM for potential further refinement, but

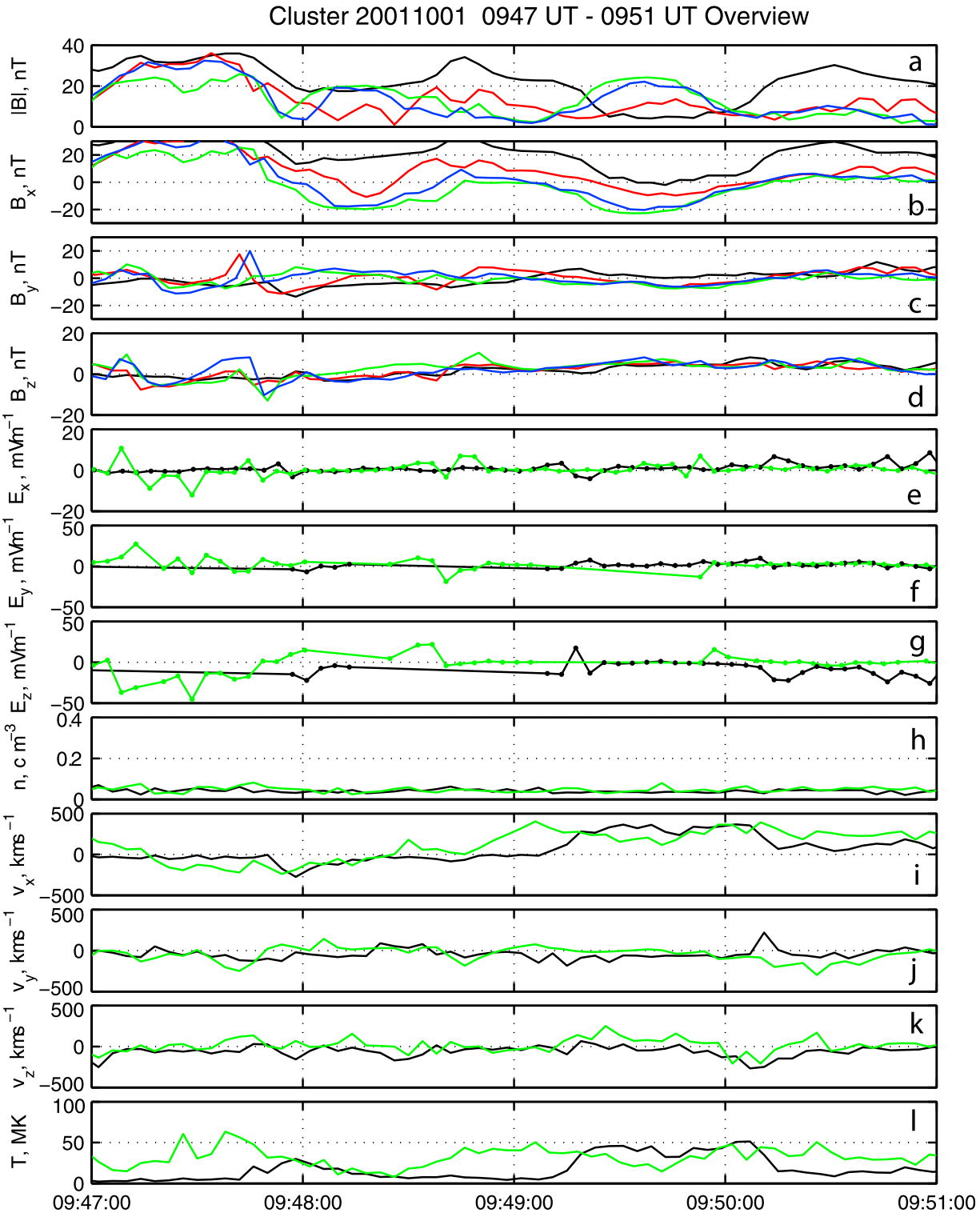

Figure 2. Cluster observations (1: black, 2: red, 3: green, 4: blue) on 1 October 2001. (a–d) Magnetic field measured by FGM. (e–g) Electric field measured by EFW. (h–l) Ion plasma moments measured by CIS-HIA.

this must be investigated in detail on a case-by-case basis after identification.

[17] Figure 2 shows an overview plot of event M, which is the extensively studied diffusion region observed on 1 October 2001 0947 UT–0951 UT [*Runov et al.*, 2003; *Cattell et al.*, 2005; *Wygant et al.*, 2005; *Imada et al.*, 2007; *Chen et al.*, 2008]. During this interval v_x (Figure 2i) reversed from negative to positive values. At the same time, B_z (Figure 2d) also reversed from negative to positive values. Cluster 3 was closest to the Earth and Cluster 4 farthest

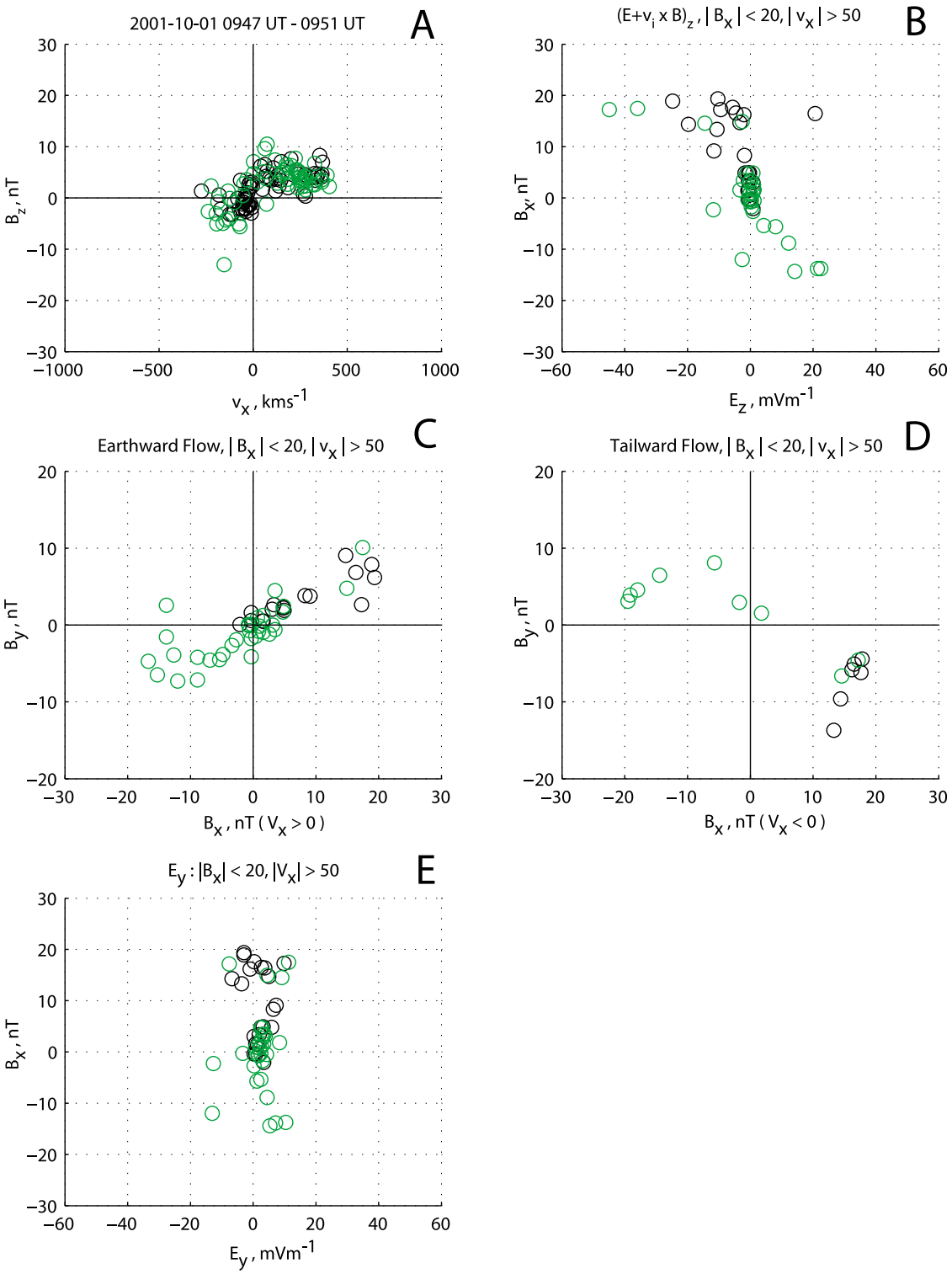

Figure 3. (a) Correlation of B_z and v_x. (b) Correlation of B_x and $(E + v_i \times B)_z$; Hall physics predicts that these quantities should be anticorrelated. (c and d) Correlation of B_y and B_x for earthward and tailward flow. Hall physics predicts these quantities should be correlated and anticorrelated, respectively. (e) B_x as a function of E_y.

from the Earth. At 0948:30 UT, Cluster 3 observed positive B_z (and positive v_x), whereas Cluster 4 observed negative B_z. Cluster 1, also tailward of Cluster 3 observed negative B_z and weak tailward flow. This indicates that the flow reversal corresponds to a single X line moving tailward over the spacecraft.

[18] Figure 3 shows the correlation of various components of **B**, **E**, and **v**. Except for Figure 3a, we have only

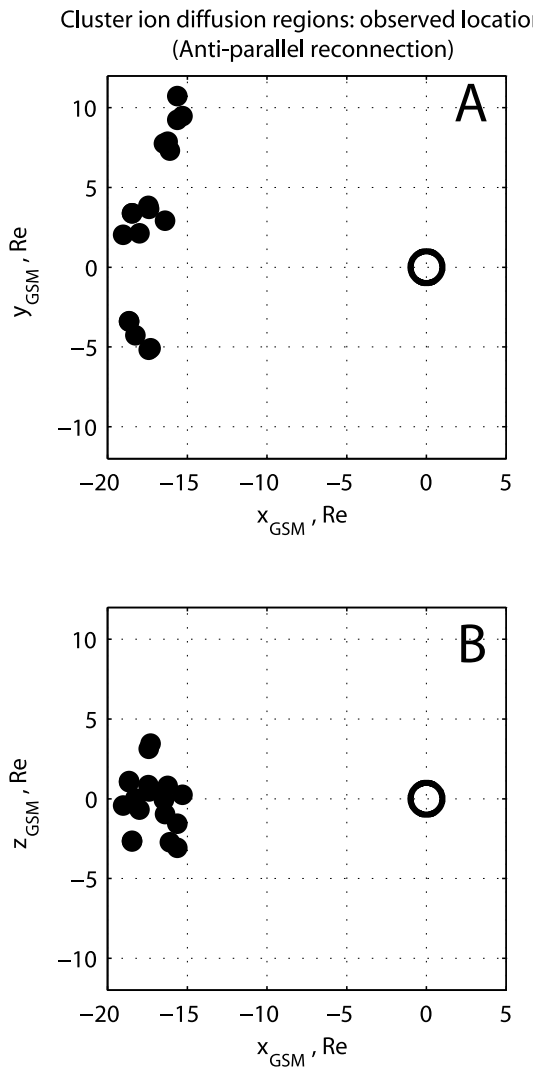

Figure 4. Location of Cluster diffusion regions associated with antiparallel reconnection: (a) *x*-*y* plane and (b) *x*-*z* plane.

shown points where $|B_x| < 20$ nT and $|v_x| > 50$ km s^{-1}. This ensures that only observations made close to the current sheet and embedded in the reconnection jet are shown. Figure 3a shows the correlation between v_x and B_z discussed in the previous paragraph. Figure 3b shows the correlation between B_x and $(\mathbf{E} + \mathbf{v}_i \times \mathbf{B})_z$. This corresponds to the electric field in the frame of the ion plasma, as given by the generalized Ohm's law:

$$\mathbf{E} + \mathbf{v}_i \times \mathbf{B} = \frac{1}{ne}\mathbf{j} \times \mathbf{B} - \frac{1}{ne}\nabla \cdot \mathbf{P}_e - \frac{m_e}{e}\frac{d\mathbf{v}_e}{dt} + \eta \mathbf{j}. \quad (1)$$

In the context of the expected structure of the ion diffusion region, $(\mathbf{E} + \mathbf{v}_i \times \mathbf{B})_z$ is mainly thought to be due to the Hall term and is expected to have a bipolar structure such that it points into the current sheet on both sides [*Wygant et al.*, 2005; *Borg et al.*, 2005; *Eastwood et al.*, 2007, 2009], as observed here. Figures 3c and 3d show the correlation between B_x and B_y for earthward and tailward flow, respectively. Referring to Figure 1, we expect that during earthward flow, $B_y > 0$ if $B_x > 0$ and $B_y < 0$ if $B_x < 0$. The opposite correlation is expected for tailward flow. Evidently the pattern is consistent with Hall magnetic fields, as reported by *Runov et al.* [2003]. Finally, Figure 3e shows the correlation between E_y and B_x. Again referring to Figure 1, we expect that E_y should be positive throughout this interval.

[19] This event is qualitatively consistent with an encounter of the ion diffusion region. To quantify its properties, a set of seven average values were calculated; the average $E_{\mathrm{Hall},z}$ for $B_x > 0$ and $B_x < 0$, the average Hall magnetic field in each of the four quadrants, and the average reconnection electric field. Furthermore, the peak values (either most positive or most negative depending on the expected signature) were also calculated. However, to minimize the influence of outliers and to mimic the possible operation of a burst trigger on a mission like MMS, the average of the top four values was calculated in each case. We have not used linear regression to calculate correlation coefficients, since although the hall fields are correlated with B_x, they are not expected to exhibit linear dependence.

[20] Each of the 33 events was examined in a similar manner for qualitative consistency with the expected pattern of Hall fields; the results are summarized in Table 2. In 18 cases, the observed correlations, and the signs of E_z and B_y, were consistent with Hall field structure. In 5 cases (events A, H, I, U, and X), there were too few data points to allow any firm conclusion to be reached. In 5 other cases (events D, W, Z, AD and AE), the observed correlations of the Hall magnetic field were completely inconsistent with the predicted morphology. In these cases, the X-line encounter essentially occurred on one side of the current sheet (i.e., $B_x > 0$ throughout, for example), and $(\mathbf{E} + \mathbf{v}_i \times \mathbf{B})_z$ was found to be close to zero throughout, except for event AE, which was found to exhibit a guide field. A more in-depth study is required to understand the details of this event. Event Z is the multiple X-line event observed on 2 October 2003 and discussed above [*Eastwood et al.*, 2005]. In these five cases, the fact that the spacecraft did not cross the current sheet, and did not observe a Hall electric field, suggests that they remained outside the diffusion region, being too far from the current sheet (along the *z* direction) to observe the Hall magnetic field pattern.

[21] In the remaining 5 cases, it was found that while the sign of the Hall magnetic field perturbation did not change as v_x or B_x changed sign, its magnitude did appear to change in a manner consistent with the expected Hall pattern. We interpret these events as reconnection occurring in the presence of a guide field whose magnitude is comparable to the Hall perturbation [*Huba*, 2005], and they remain the subject of future study. In the remainder of this paper, we will discuss the properties of the 18 events whose Hall magnetic and electric field perturbations were qualitatively consistent with the expected pattern of antiparallel reconnection.

4. Average Properties of the Ion Diffusion Region

[22] The locations of the 18 confirmed diffusion region encounters are shown in Figure 4. This shows that reconnection diffusion regions were observed between 15 and 20 Re from the Earth, within 5 Re of $z_{GSM} = 0$, and more often on the premidnight side of the magnetotail. However, these data are a strong function of the Cluster orbit, and so one should be careful when drawing conclusions about the

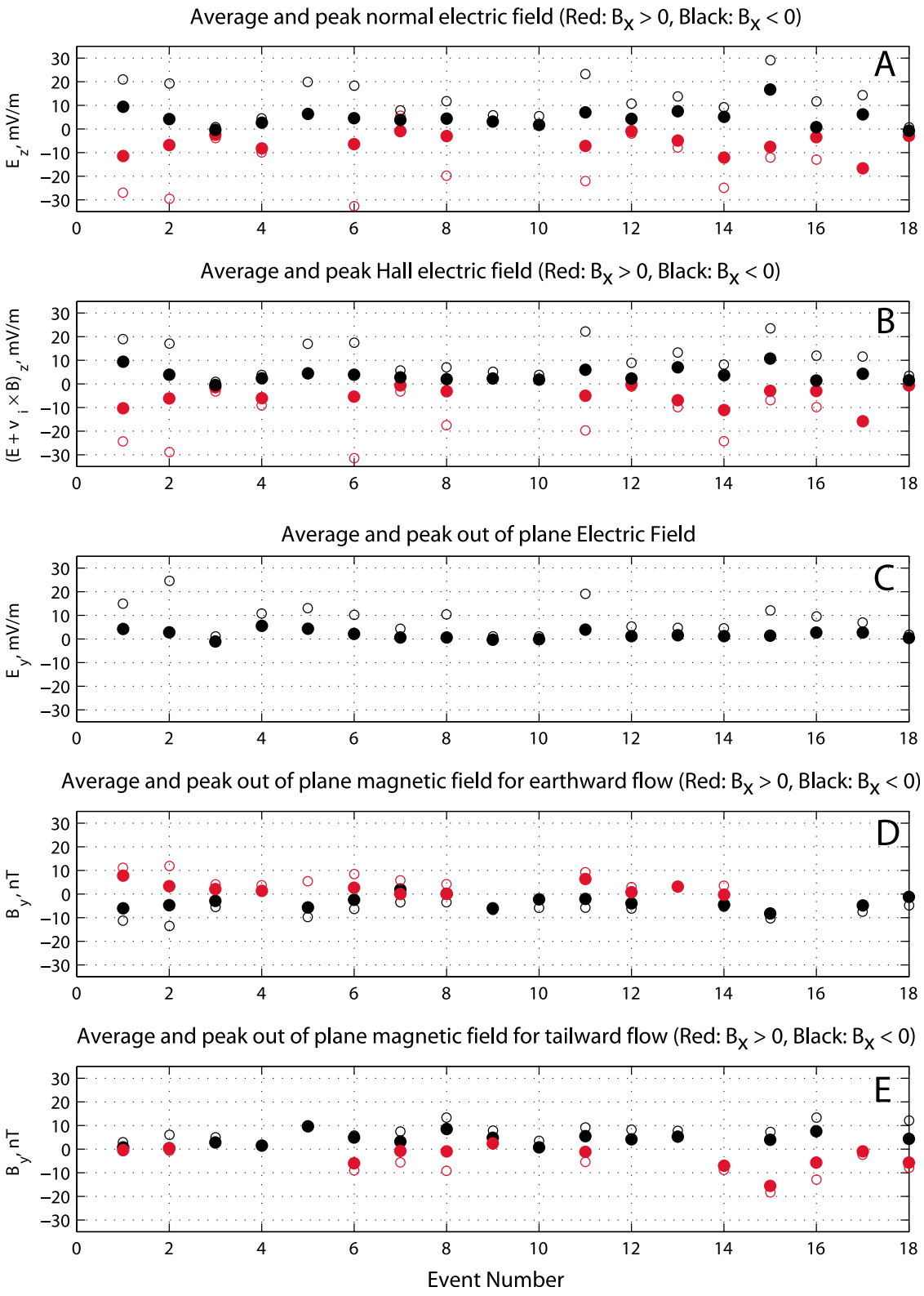

Figure 5. Average (solid points) and peak (open circles) values of (a) the normal electric field (b) the Hall electric field $(E + v_i \times B)_z$, (c) the out of plane electric field E_y, (d) the out of plane Hall magnetic field during earthward flow, and (e) the out of plane Hall magnetic field during tailward flow. For Figures 5a, 5b, 5d, and 5e, red and black points correspond to $B_x > 0$ and $B_x < 0$.

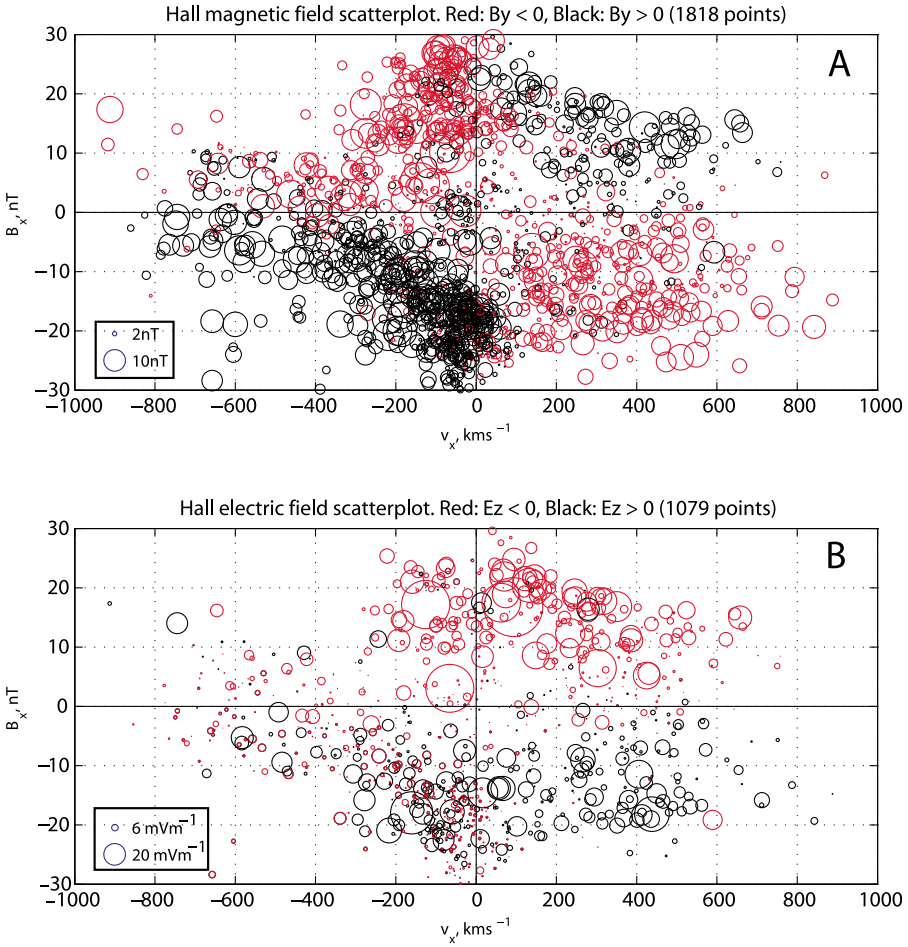

Figure 6. (a) Out of plane magnetic field B_y as a function of B_x and v_x. Black corresponds to $B_y > 0$ and red corresponds to $B_y < 0$. (b) $(E + v_i \times B)_z$ as a function of B_x and v_x. Black corresponds to $E_z > 0$ and red corresponds to $E_z < 0$. In each scatterplot the size of the circle corresponds to the magnitude of the data point.

most typical location of the diffusion region, although we note that similar asymmetries in the location of flow reversal events further downtail [*Nagai et al.*, 1998; *Asano et al.*, 2004] and bursty bulk flows [*Raj et al.*, 2002] have been reported.

[23] For each of the 18 events, the 14 average and peak parameters described in the previous section were calculated and are shown in Figure 5. In addition, Figure 5a shows the properties of the normal electric field E_z and Figure 5b shows $(\mathbf{E} + \mathbf{v}_i \times \mathbf{B})_z$ for all 18 events; solid circles correspond to the average values and open circles to the peak values. Red indicates $B_x > 0$, and black indicates $B_x < 0$. Missing points show that there were no observations in that particular hemisphere; for example, in event #10, the flow reversal was observed entirely in the Northern Hemisphere. The difference between E_z and $(\mathbf{E} + \mathbf{v}_i \times \mathbf{B})_z$ is relatively small. It can be seen that the red points ($B_x > 0$; above the current sheet in Figure 1) all correspond to negative normal electric fields and that the black points ($B_x < 0$; below the current sheet in Figure 1) all correspond to positive normal electric fields, indicating the persistence of the Hall electric field pattern. Figure 5c shows out of plane electric field, E_y. Again, the solid circles show the average value in each event, and the open circles show the peak value. Under ideal circumstances, E_y corresponds to the reconnection electric field E_r, which is expected to be positive. We find that in only three of these events is the average E_y negative. However, it is important to bear in mind that the relationship between E_y and E_r is not trivial. Even a small tilt of the current sheet in the *Y-Z* plane can cause E_y to be contaminated by E_z, which is large. The flapping motion of the current sheet in the *Z* direction and the motion of the X line in the *X* direction must also be accounted for. Combined with the ~1 mV m^{-1} experimental uncertainty in the electric field, this means that E_r is one of the most difficult parameters to measure. Figure 5d shows the out-of-plane (Hall) magnetic field for earthward flow. In the Earthward flow above the current sheet ($B_x > 0$, black points), we expect that B_{Hall} to be positive; below the current sheet ($B_x < 0$, red points), we expect that B_{Hall} to be negative. This is reflected by the fact that except for one event, all the red points are greater than 0, and all the black points are less than 0. Figure 5e shows equivalent data for tailward flow. In this case the pattern is reversed compared to Figure 5d.

[24] Figure 6 shows all of the data as a function of B_x and v_x. Figure 6a shows the out of plane (Hall) magnetic field data. A total of 1818 data points are shown (~121 min of observations). Note that here black and red are used in a different way: Black corresponds to $B_y > 0$ and red

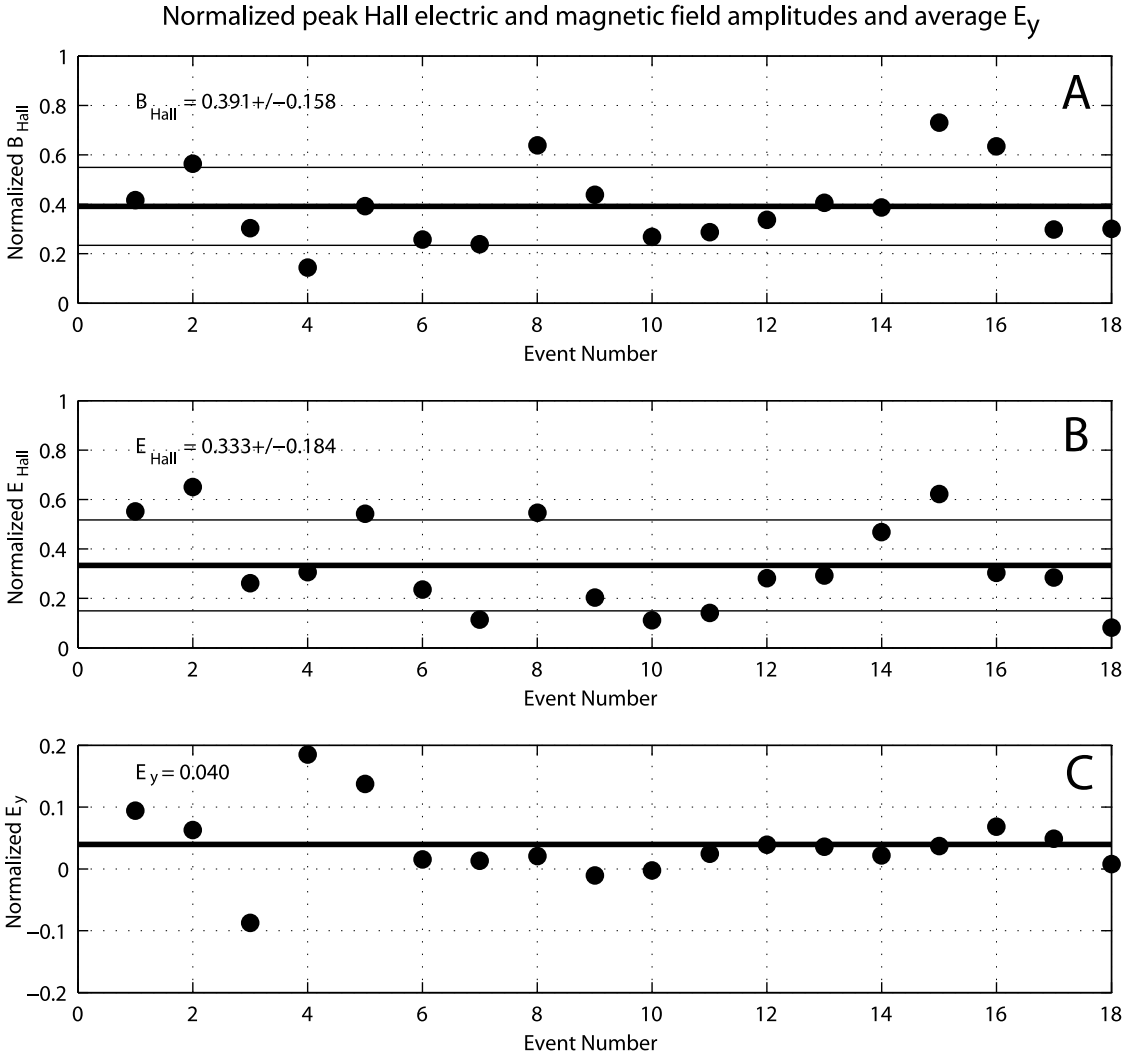

Figure 7. (a) peak Hall magnetic field; (b) peak Hall electric field; (c) average out-of-plane electric field E_y. All data are shown in normalized units for each event.

corresponds to $B_y < 0$. The size of the circle corresponds to the magnitude of B_y. The emergence of the quadrupole pattern is immediately apparent. Figure 6b shows the normal (Hall) electric field data. Again the colors are used differently: Black corresponds to $E_z > 0$ and red corresponds to $E_z < 0$, with the size of the circle corresponding to the magnitude of E_z. Although fewer data points (1079, ~72 min of observations) are shown here, because of the restrictions of the reconstruction of **E** described in section 2, the emergence of a bipolar pattern is again apparent. The emergence of these patterns shows that when attempting to identify and study diffusion regions in the magnetotail, it is reasonable to use the GSM coordinate system in the first instance, and any localized current sheet tilting or warping does not appear to lead to any sort of systematic overall deviation of the geometry from GSM.

5. Normalization and Comparison With Simulations

[25] While Figure 5 shows the qualitatively consistency of the Hall field structure from event to event, there is considerable scatter in the quantitative values observed. To better understand this, the absolute maximum of the four peak values of the Hall magnetic field was calculated for each event, together with the absolute maximum of the two peak values of the Hall electric field. These values were then normalized; the peak Hall magnetic field was normalized to the magnetic field just outside the reconnection region, B_{inflow} such that $b_{\mathrm{H}} = B_{\mathrm{Hall}}/B_{\mathrm{inflow}}$. The peak Hall electric field was normalized to the density observed at the center of the current sheet n_{cs} and the inflow magnetic field B_{inflow}, such that $e_{\mathrm{H}} = E_{\mathrm{Hall}}/(B_{\mathrm{inflow}} \times V_A(n_{\mathrm{cs}}, B_{\mathrm{inflow}}))$, where V_A is the Alfvén speed constructed from n_{cs} and B_{inflow}. The normalized values are shown in Figure 7; thick horizontal lines show the mean value, and the thin horizontal lines show the standard deviation. The peak normalized Hall magnetic field is 0.39 ± 0.16, and the peak normalized Hall electric field is 0.33 ± 0.18.

[26] Having established these values, we compare them to the results of computer simulations. Numerous simulations of magnetic reconnection have been performed by many research groups using a variety of different codes.

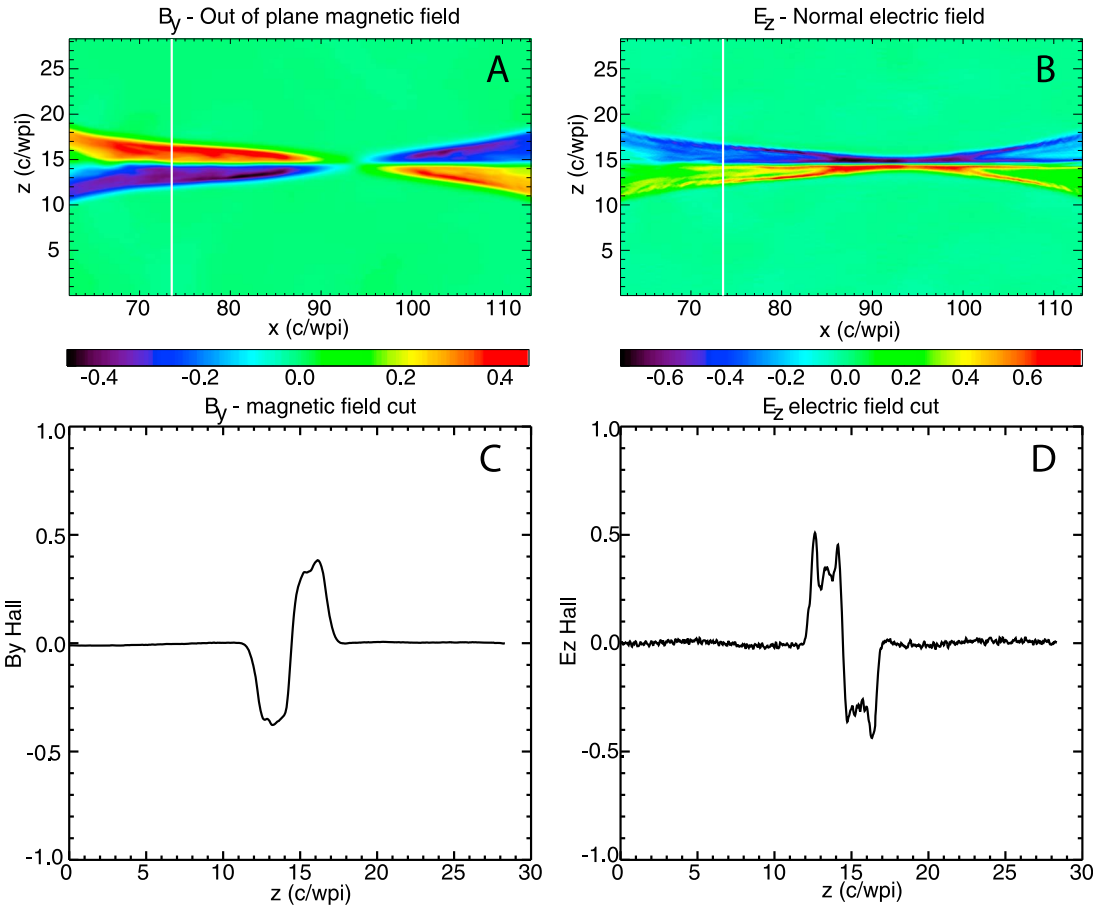

Figure 8. (a and b) PIC simulation of magnetic reconnection showing the structure of the out of plane magnetic field and the normal electric field. (c and d) the out of plane magnetic field and the normal electric field along a cut through the exhaust shown by the white line in Figures 8a and 8b.

However, to ensure similar renormalization of the simulation data and enable accurate comparison with the observational data, a simulation of magnetic reconnection was performed using the particle in cell code P3D [*Zeiler et al.*, 2002]. The exact properties of the simulation are described in *Shay et al.* [2007]; to summarize here, the simulation was performed in 2.5 dimensions (two space dimensions here labeled X and Z to correspond to the geometry of the magnetotail and three-dimensional fields, with $\partial/\partial y = 0$). A mass ratio $m_i/m_e = 25$ was used, with $T_e = 1/12$ and $T_i = 5/12$. The simulation has been renormalized to the density at the center of the current sheet and the inflow magnetic field strength in the same way as the experimental data. Using this renormalization the system size is $115.86 \times 57.9\ c/w_{pi}$, with periodic boundaries. The system was initialized with no guide field and two Harris current sheets superimposed on background density of 0.2. Figure 8a shows the out of plane Hall magnetic field and Figure 8b shows the normal (Hall) electric field which except at the central current sheet is due to Hall physics [*Karimabadi et al.*, 2007; *Shay et al.*, 2007; *Phan et al.*, 2007; *Drake et al.*, 2008]. Only a small region of the simulation centered on one of the X lines at a time when reconnection has been established is shown.

[27] The patterns in the Hall magnetic and electric field are consistent with both the theoretical picture in Figure 1 and the data shown in Figure 6. Figures 8c and 8d show the out of plane magnetic field and the normal electric field along a vertical cut through the left hand exhaust. (The cut is shown as a white line in the top panels; the location of the cut is not of specific importance and is shown for illustration to help the reader translate between the colors and the actual numerical values.) The peak Hall magnetic field is ~0.4 and the peak Hall electric field is between ~0.3–0.5, consistent with the observations. The sizes of these peak values are relatively insensitive to the location of the cut in the x direction (as can be seen from the relatively uniform colors in the quadrants of Figure 8a. We note that the Hall magnetic field is slightly larger than in previous studies [*Birn et al.*, 2001] and that there is spread in simulation results, perhaps due to the different parameters used.

[28] Finally, for completeness, we consider the reconnection electric field and E_y. Since theoretically the reconnection electric field is uniform and constant during steady-state reconnection, the average value of E_y has been normalized such that $e_y = E_y/[B_{\text{inflow}} \times V_A(n_{\text{cs}}, B_{\text{inflow}})]$. It is important to note that the since the reconnection electric field is small, typically only a few mV m^{-1}, it is difficult to measure because of uncertainties in the precise orientation of the X line, the flapping of the current sheet (where motion of

the current sheet in the z_{GSM} direction will be associated with a varying E_y), the motion of the X line, and the resolution of the data. These effects combine to "contaminate" E_y and generate scatter in the measured values. Figure 7c shows that the average value of E_y is found to be 0.04, although it can be as high as ~0.2. In the simulation, the normalized reconnection electric field was found to be 0.1. This indicates that reconnection in the magnetotail is typically fast.

6. Conclusions

[29] The Cluster magnetotail data set from 2001–2005 has been searched for encounters with the ion diffusion region. A survey for correlated reversals in v_x and B_z while in the plasma sheet resulted in a set of 33 events. Of the events amenable to multispacecraft analysis, all but 1 were consistent with a single X line moving over the spacecraft. Most of the events corresponded to an X line retreating tailward. In two cases, two distinct X lines were observed a few minutes apart; together with the O-line encounter this suggests that multiple X-line reconnection, while observationally quite rare, does occur in the magnetotail.

[30] These events were then examined for the presence of Hall electric and magnetic fields. Eighteen events were found to exhibit electric and magnetic field perturbations qualitatively consistent with the predictions of antiparallel Hall reconnection. In 5 events, there were too few data points to allow any firm conclusion to be reached. In 5 other cases, no Hall electric field perturbation was observed and the correlations of the Hall magnetic field were completely inconsistent with the predicted morphology, suggesting that they remained outside the diffusion region. In the remaining 5 cases, while the sign of the Hall magnetic field perturbation did not change as v_x or B_x reversed, its magnitude did appear to change in a manner consistent with the expected Hall pattern. We interpret these events as reconnection occurring in the presence of a guide field; these events remain the subject of future study. This result shows that diffusion region encounters are indeed relatively rare, but if one observes a field and flow reversal, there is a reasonable chance that one will also encounter the diffusion region. However, this is a function of the spacecraft orbit and in particular the apogee. We also note that it appears to be sufficient to analyze the data in the GSM coordinate system, although further refinement in individual cases may be possible by examining the data more carefully.

[31] The 18 events exhibiting qualitative consistency with the predictions of Hall reconnection were further studied to establish on a more quantitative basis the size of the Hall electric and magnetic fields. The average value and the peak value (based on the average of the top four measurements) in each quadrant/hemisphere of the magnetic/electric field were calculated for each event. The peak Hall magnetic and electric field in each of these 18 events was then normalized using the inflow magnetic field and the current sheet number density. This resulted in an average peak Hall magnetic field of 0.39 ± 0.16 and an average peak Hall electric field of 0.33 ± 0.18. While there is scatter among the events, this gives an experimental value for the size of the Hall fields, peaking between 1/3 and 1/2 in normalized units. The normalized average value of the out of plane electric field E_y was found to be 0.04 but was as high as ~0.2 in individual events. (In fact the event with the largest reconnection rate was previously found to have a reconnection rate of 0.07–0.15 using a different method of calculation [*Xiao et al.*, 2007].) We caution, however, that converting measurements of E_y to the reconnection electric field is in general difficult because of sensitivity to the exact geometry of the X line and its motion and errors associated with the underlying measurements. Nevertheless, while the data must be interpreted with care, the events are still in general consistent with fast reconnection. These results were found to be in close agreement with the predictions of a PIC simulation of reconnection, similarly normalized, and show that when observed, the pattern of Hall electric and magnetic fields in the vicinity of a field and flow reversal in the magnetotail is quantitatively consistent with the predictions of simulations.

[32] Finally, although the diffusion region is difficult to encounter, and the main flow reversal typically lasts a few minutes (although this is embedded in a longer interval of tailward and/or earthward flow), one of the most significant signatures is in fact the total DC electric field (which is in large part dominated by the Hall electric field), which can attain peak values of several tens of millivolts per meter. This suggests that in both present and future missions, the total DC electric field may be a useful tool for automatically identifying encounters with the diffusion region in the data.

[33] **Acknowledgments.** This work was supported by NASA grants NNX07AF32G, NNX08AM37G, and NNX08AO83G and has made use of the Cluster Active Archive. Simulations were carried out at the National Energy Research Scientific Computing Center. J.P.E. holds a STFC Advanced Fellowship at I.C.L.

[34] Philippa Browning thanks Rumi Nakamura and Tsugunobu Nagai for their assistance in evaluating this manuscript.

References

Alexeev, I. V., C. J. Owen, A. N. Fazakerley, A. Runov, J. P. Dewhurst, A. Balogh, H. Rème, B. Klecker, and L. M. Kistler (2005), Cluster observations of currents in the plasma sheet during reconnection, *Geophys. Res. Lett.*, *32*, L03101, doi:10.1029/2004GL021420.

Asano, Y., T. Mukai, M. Hoshino, Y. Saito, H. Hayakawa, and T. Nagai (2004), Current sheet structure around the near-Earth neutral line observed by Geotail, *J. Geophys. Res.*, *109*, A02212, doi:10.1029/2003JA010114.

Asano, Y., et al. (2008), Electron flat-top distributions around the magnetic reconnection region, *J. Geophys. Res.*, *113*, A01207, doi:10.1029/2007JA012461.

Balogh, A., et al. (2001), The Cluster magnetic field investigation: Overview of inflight performance and initial results, *Ann. Geophys.*, *19*, 1207–1217.

Baumjohann, W. (1993), The near-Earth plasma sheet: An AMPTE-IRM perspective, *Space Sci. Rev.*, *64*, 141–163.

Baumjohann, W., G. Paschmann, and H. Luhr (1990), Characteristics of high-speed ion flows in the plasma sheet, *J. Geophys. Res.*, *95*(A4), 3801–3809.

Birn, J., et al. (2001), Geospace Environmental Modeling (GEM) magnetic reconnection challenge, *J. Geophys. Res.*, *106*(A3), 3715–3719.

Birn, J., J. Raeder, Y. L. Wang, R. A. Wolf, and M. Hesse (2004), On the propagation of bubbles in the geomagnetic tail, *Ann. Geophys.*, *22*, 1773–1786.

Borg, A. L., M. Øieroset, T. Phan, F. S. Mozer, A. Pedersen, C. Mouikis, J. P. McFadden, C. Twitty, A. Balogh, and H. Rème (2005), Cluster encounter of a magnetic reconnection diffusion region in the near-Earth magnetotail on September 19, 2003, *Geophys. Res. Lett.*, *32*, L19105, doi:10.1029/2005GL023794.

Cattell, C. A., et al. (2005), Cluster observations of electron holes in association with magnetotail reconnection and comparison to simulations, *J. Geophys. Res.*, *110*, A01211, doi:10.1029/2004JA010519.

Chen, L.-J., et al. (2008), Observation of energetic electrons within magnetic islands, *Nat. Phys.*, *4*, 19–23.

Drake, J. F., M. A. Shay, and M. Swisdak (2008), The Hall fields and fast magnetic reconnection, *Phys. Plasmas*, *15*, 042306.

Dungey, J. W. (1961), Interplanetary magnetic field and the auroral zones, *Phys. Rev. Lett.*, *6*, 47–48.

Eastwood, J. P., D. G. Sibeck, J. A. Slavin, M. L. Goldstein, B. Lavraud, M. Sitnov, S. Imber, A. Balogh, E. A. Lucek, and I. Dandouras (2005), Observations of multiple X-line structure in the Earth's magnetotail current sheet: A Cluster case study, *Geophys. Res. Lett.*, *32*, L11105, doi:10.1029/2005GL022509.

Eastwood, J. P., T.-D. Phan, F. S. Mozer, M. A. Shay, M. Fujimoto, A. Retinò, M. Hesse, A. Balogh, E. A. Lucek, and I. Dandouras (2007), Multi-point observations of the Hall electromagnetic field and secondary island formation during magnetic reconnection, *J. Geophys. Res.*, *112*, A06235, doi:10.1029/2006JA012158.

Eastwood, J. P., T. D. Phan, S. D. Bale, and A. Tjulin (2009), Observations of turbulence generated by magnetic reconnection, *Phys. Rev. Lett.*, *102*, 035001.

Escoubet, C. P., M. Fehringer, and M. L. Goldstein (2001), The Cluster mission, *Ann. Geophys.*, *19*, 1197–1200.

Fairfield, D. H., and L. J. Cahill (1966), Transition region magnetic field and polar magnetic disturbances, *J. Geophys. Res.*, *71*(1), 155–169.

Fujimoto, M., M. S. Nakamura, I. Shinohara, T. Nagai, T. Mukai, Y. Saito, T. Yamamoto, and S. Kokubun (1997), Observations of earthward streaming electrons at the trailing boundary of a plasmoid, *Geophys. Res. Lett.*, *24*(22), 2893–2896, doi:10.1029/97GL02821.

Gustafsson, G., et al. (2001), First results of electric field and density observations by Cluster EFW based on initial months of operation, *Ann. Geophys.*, *19*, 1219–1240.

Henderson, P. D., C. J. Owen, A. D. Lahiff, I. V. Alexeev, A. N. Fazakerley, E. A. Lucek, and H. Rème (2006), Cluster PEACE observations of electron pressure tensor divergence in the magnetotail, *Geophys. Res. Lett.*, *33*, L22106, doi:10.1029/2006GL027868.

Huba (2005), Hall magnetic reconnection: Guide field dependence, *Phys. Plasmas*, *12*, 012322.

Imada, S., R. Nakamura, P. Daly, M. Hoshino, W. Baumjohann, S. Mühlbachler, A. Balogh, and H. Rème (2007), Energetic electron acceleration in the downstream reconnection outflow region, *J. Geophys. Res.*, *112*, A03202, doi:10.1029/2006JA011847.

Karimabadi, H., W. Daughton, and J. Scudder (2007), Multi-scale structure of the electron diffusion region, *Geophys. Res. Lett.*, *34*, L13104, doi:10.1029/2007GL030306.

Laitinen, T. V., R. Nakamura, A. Runov, H. Rème, and E. A. Lucek (2007), Global and local disturbances in the magnetotail during reconnection, *Ann. Geophys.*, *25*, 1025–1035.

Mozer, F. S., S. D. Bale, and T. D. Phan (2002), Evidence of diffusion regions at a subsolar magnetopause crossing, *Phys. Rev. Lett.*, *89*, 015002.

Nagai, T., M. Fujimoto, Y. Saito, S. Machida, T. Terasawa, R. Nakamura, T. Yamamoto, T. Mukai, A. Nishida, and S. Kokubun (1998), Structure and dynamics of magnetic reconnection for substorm onsets with Geotail observations, *J. Geophys. Res.*, *103*(A3), 4419–4440.

Nagai, T., I. Shinohara, M. Fujimoto, M. Hoshino, Y. Saito, S. Machida, and T. Mukai (2001), Geotail observations of the Hall current system: Evidence of magnetic reconnection in the magnetotail, *J. Geophys. Res.*, *106*(A11), 25,929–25,949.

Nagai, T., I. Shinohara, M. Fujimoto, S. Machida, R. Nakamura, Y. Saito, and T. Mukai (2003), Structure of the Hall current system in the vicinity of the magnetic reconnection site, *J. Geophys. Res.*, *108*(A10), 1357, doi:10.1029/2003JA009900.

Nagai, T., M. Fujimoto, R. Nakamura, W. Baumjohann, A. Ieda, I. Shinohara, S. Machida, Y. Saito, and T. Mukai (2005), Solar wind control of the radial distance of the magnetic reconnection site in the magnetotail, *J. Geophys. Res.*, *110*, A09208, doi:10.1029/2005JA011207.

Nakamura, R., W. Baumjohann, Y. Asano, A. Runov, A. Balogh, C. J. Owen, A. N. Fazakerley, M. Fujimoto, B. Klecker, and H. Reme (2006), Dynamics of thin current sheets associated with magnetotail reconnection, *J. Geophys. Res.*, *111*, A11206, doi:10.1029/2006JA011706.

Øieroset, M., T. D. Phan, M. Fujimoto, R. P. Lin, and R. P. Lepping (2001), In situ detection of collisionless reconnection in the Earth's magnetotail, *Nature*, *412*, 414–417.

Østgaard, N. S. K., A. L. Borg, A. Aasnes, A. Pedersen, M. Øieroset, T. Phan, and S. E. Haaland (2009), Can magnetotail reconnection produce the auroral intensities observed in the conjugate ionosphere?, *J. Geophys. Res.*, *114*, A06204, doi:10.1029/2009JA014185.

Paschmann, G. (2008), Recent in-situ observations of magnetic reconnection in near-Earth space, *Geophys. Res. Lett.*, *35*, L19109, doi:10.1029/2008GL035297.

Phan, T. D., J. F. Drake, M. A. Shay, F. S. Mozer, and J. P. Eastwood (2007), Evidence for an elongated (>60 ion skin depths) electron diffusion region during fast magnetic reconnection, *Phys. Rev. Lett.*, *99*, 255002.

Raj, A., T. Phan, R. P. Lin, and V. Angelopoulos (2002), Wind survey of high-speed bulk flows and field-aligned beams in the near-Earth plasma sheet, *J. Geophys. Res.*, *107*(A12), 1419, doi:10.1029/2001JA007547.

Rème, H., et al. (2001), First multispacecraft ion measurements in and near the Earth's magnetosphere with the identical Cluster ion spectrometry (CIS) experiment, *Ann. Geophys.*, *19*, 1303–1354.

Runov, A., et al. (2003), Current sheet structure near magnetic X-line observed by Cluster, *Geophys. Res. Lett.*, *30*(11), 1579, doi:10.1029/2002GL016730.

Runov, A., et al. (2008), Observations of an active thin current sheet, *J. Geophys. Res.*, *113*, A07S27, doi:10.1029/2007JA012685.

Schwartz, S. J. (1998), Shock and discontinuity normals, mach numbers and related parameters, in *Analysis Methods for Multi-Spacecraft Data*, edited by G. Paschmann and P. W. Daly, pp. 249–270, International Space Science Institute, Bern.

Shay, M. A., J. F. Drake, R. E. Denton, and D. Biskamp (1998), Structure of the dissipation region during collisionless magnetic reconnection, *J. Geophys. Res.*, *103*(A5), 9165–9176.

Shay, M. A., J. F. Drake, and M. Swisdak (2007), Two-scale structure of the electron dissipation region during collisionless magnetic reconnection, *Phys. Rev. Lett.*, *99*, 155002.

Sonnerup, B. U. Ö. (1979), Magnetic field reconnection, in *Solar System Plasma Physics Volume III*, edited by L. T. Lanzerotti, C. F. Kennel, and E. N. Parker, pp. 47–108, North-Holland, Amsterdam.

Ueno, G., S. Machida, T. Mukai, Y. Saito, and A. Nishida (1999), Distribution of X-type magnetic neutral lines in the magnetotail with Geotail observations, *Geophys. Res. Lett.*, *26(22)*, 3341–3344, doi:10.1029/1999GL010714.

Wygant, J. R., et al. (2005), Cluster observations of an intense normal component of the electric field at a thin reconnecting current sheet in the tail and its role in the shock-like acceleration of the ion fluid into the separatrix region, *J. Geophys. Res.*, *110*, A09206, doi:10.1029/2004JA010708.

Xiao, C. J., et al. (2007), A Cluster measurement of fast magnetic reconnection in the magnetotail, *Geophys. Res. Lett.*, *34*, L01101, doi:10.1029/2006GL028006.

Zeiler, A., D. Biskamp, J. F. Drake, B. N. Rogers, and M. A. Shay (2002), Three-dimensional particle simulations of collisionless magnetic reconnection, *J. Geophys. Res.*, *107*(A9), 1230, doi:10.1029/2001JA000287.

J. P. Eastwood, Blackett Laboratory, Imperial College London, Prince Consort Road, London SW7 2AZ, UK. (jonathan.eastwood@imperial.ac.uk)

M. Øieroset and T. D. Phan, Space Sciences Laboratory, University of California, Grizzly Peak Blvd. at Centennial Dr., Berkeley, CA 94720, USA.

M. A. Shay, Department of Physics and Astronomy, Bartol Research Institute, University of Delaware, 104 The Green, 217 Sharp Lab, Newark, DE 19716, USA.